Emam et al. 2018. *Int. J. Vehicle Structures & Systems*, 10(4), 300-306
ISSN: 0975-3060 (Print), 0975-3540 (Online)
doi: 10.4273/ijvss.10.4.15

International Journal of Vehicle Structures & Systems
Available online at www.maftree.org/eja

Optimized Fractional-Order Proportional Integral Derivative Controller for Active Vehicle Suspension System Performance Enhancement

A.S. Emam[a,b], H. Metered[a,c] and A.M. Abdel Ghany[d]

[a]*Automotive & Tractors Engineering Dept., Faculty of Engg., Mataria, Helwan University, Cairo, Egypt*
[b]*Corresponding Author, Email: ashrafgalab71@gmail.com*
[c]*Email: hassan.metered@yahoo.com*
[d]*Electrical Power & Machine Dept., Faculty of Engg., Helwan, Helwan University, Cairo, Egypt*
Email: ghayghany@hotmail.com

ABSTRACT:

In this paper, an optimal Fractional Order Proportional Integral Derivative (FOPID) controller is applied in vehicle active suspension system to improve the ride comfort and vehicle stability without consideration of the actuator. The optimal values of the five gains of FOPID controller to minimize the objective function are tuned using a Multi-Objective Genetic Algorithm (MOGA). A half vehicle suspension system is modelled mathematically as 6 degrees-of-freedom mechanical system and then simulated using Matlab/Simulink software. The performance of the active suspension with FOPID controller is compared with passive suspension system under bump road excitation to show the efficiency of the proposed controller. The simulation results show that the active suspension system using the FOPID controller can offer a significant enhancement of ride comfort and vehicle stability.

KEYWORDS:

Half vehicle active suspension; Fractional order PID controller; Multi-objective genetic algorithm; Ride comfort

CITATION:

A.S. Emam, H. Metered and A.M. Abdel Ghany. 2018. Optimized Fractional-Order Proportional Integral Derivative Controller for Active Vehicle Suspension System Performance Enhancement, *Int. J. Vehicle Structures & Systems*, 10(4), 300-306. doi:10.4273/ijvss.10.4.15.

1. Introduction

Active and semi-active suspensions have been widely investigated during past few decades and a lot of control strategies have been applied. Suspension system is one of the most essential components of vehicle which plays a vital role related to ride comfort, vehicle stability and vehicle chassis altitude. The main purposes of suspension systems are to isolate the vehicle body from road surface irregularities to maximize passenger comfort and maintain sufficient continuous road tyre-contact to grant vehicle stability [1]. Actually, it is challenging issue for suspension system to simultaneously improve all performance criteria using a simple control technique. So that, the design of active or semi-active suspension has trade-offs between comfort and stability which the controller has to solve [2-3]. This trade-offs can be solved by the integration between simple or complicated control techniques and optimization algorithms to minimize good objective functions related to suspension performance criteria measured by few sensors to feedback the controller with appropriate inputs to compute the optimum actuator force [4-5].

There are three main categories of suspension systems; passive, semi-active, and active suspension. In passive suspension, elastic and damping characteristics of springs and dampers remain constant and have performance limitations over working frequency range. Active suspension systems are more changeable, efficient and effective in enhancing suspension performance than passive systems and semi-active as well. In active vehicle suspensions, the external road excitation is dissipated by the generation of a control force based on the vehicle response via a moveable actuator by an external energy source [6-8]. Active suspensions are usually consists of an actuator (force source), sensors, and a controller. The actuation force is calculated dynamically as a function of measured suspension performance criteria. A wide range of control strategies have been applied to active vehicle suspensions to investigate the trade-offs between comfort and stability.

A full state feedback controller of active vehicle suspension was applied in [5] to study the effects of representation of the road surface as integrated or filtered white noise, cross-correlation between left and right track excitations and wheelbase time delay between front and rear inputs in deriving the control laws. Proportional-integral sliding mode controller was employed as a robust control approach to control the unwanted vibration of active suspension [9]. A simple adaptive feedback-linearization approach was applied for nonlinear vehicle suspension system which is excited by unknown road surface profiles. An extended observer was used to approximate the nonlinear effects. Based on the approximation, the effects of the nonlinear suspension are avoided [10]. Linear quadratic optimal controller and conventional acceleration dependent

method [11] were designed for control strategies. Adaptive fuzzy sliding-mode control is applied for nonlinear uncertain vehicle active suspension systems taking into account both actuator nonlinearity and uncertainties in vehicle suspension model [12].

Further, fuzzy logic controllers are also employed for vehicle active suspension systems; quarter model [8] and half model [13]. A study of the usage of a fuzzy based sliding surface controller which depends on the ideal sky-hook model for active suspension system is introduced to improve the ride comfort and vehicle stability [14]. H_∞ Control theory was applied for an active suspension control system to minimize the road excitation effect on the system performance criteria [15-16]. A semi-active suspension control strategy using mixed H_2/H_∞ robust technique was investigated for quarter car model to enhance the ride comfort and vehicle stability [17]. Self-tuning Proportional Integral Derivative (PID) controllers were designed using fuzzy logic of a quarter vehicle model suspension system in order to adjust the gain parameters of PID controllers and so improved the suspension performance [18-19]. PID controllers are the most popular industrial feedback controllers due to its simpler structure, cost effective, and easier in implementation. They were applied in a lot of vehicle applications such as active [20] and semi-active vehicle suspension systems [4].

Fractional order $PI^{\lambda}D^{\mu}$ (FOPID) controller was found as a general form of a classical PID controller which introduced recently to reduce vibration levels of smart base-isolated structures [21]. FOPID controllers have been greatly used and verified to offer a very good performance for active steering [22] and active suspension [23]. The former control methodology is applied in this article to enhance the overall performance of active vehicle suspension system. This paper addresses the tuning of the parameters of optimal FOPID controller by using Multi-Objective Genetic Algorithm (MOGA) in order to reduce the vibration levels of a half vehicle active suspension system by introducing a simple controller with the ability to improve all suspension system performance outputs. The MOGA is used to search the optimum values of K_p, K_i, K_d, λ and μ.

2. Half vehicle suspension system model

Fig. 1 represents a half vehicle suspension system model which has 6 degrees-of-freedom (DoF). The suspension model has three main parts; vehicle chassis/body, two axles, and two seats. It is assumed that the chassis/body has both bounce and pitch, the axles have independent bounce, and the seats have only vertical motion. The suspension, tyre, and seats are modelled using linear springs in parallel with viscous dampers as considered in [22]. Two active actuators are located parallel to the suspension elements, spring and passive damper, to provide controllable forces. By applying Newton's second law, Eqns. (1) to (6) describe a general case of which the vehicle is suspended by conventional passive dampers and two active actuators.

$$\frac{k_1}{m}x_{t1}+\frac{k_2}{m}x_{t2}+\frac{c_{p1}}{m}\dot{x}_{p1}+\frac{c_{p2}}{m}\dot{x}_{p2}+\frac{c_1}{m}\dot{x}_{t1}+\frac{c_2}{m}\dot{x}_{t2}-\frac{1}{\mathrm{m}}(\mathrm{c_1+c_2+k_{p1}+k_{p2}})\dot{\mathrm{x}}-\frac{1}{\mathrm{m}}(\mathrm{c_1b_1-c_2b_2+c_{p1}d_1-c_{p2}d_2})\dot{\theta}+\frac{\mathrm{F_{a1}+F_{a2}}}{\mathrm{m}} \quad (1)$$

$$\ddot{\theta}=\frac{1}{I_P}(k_1b_1-k_2b_2+k_{p1}d_1-k_{p2}d_2)x-\frac{1}{I_P}(k_1b_1^2-k_2b_2^2+k_{p1}d_1^2+k_{p2}d_2^2)\theta-\frac{k_{p1}d_1}{I_p}x_{p1}+\frac{k_{p2}d_2}{I_p}x_{p2}-\frac{k_1b_1}{I_p}x_{t1}+\frac{k_2b_2}{I_p}x_{t2}-\frac{1}{I_P}(c_1b_1-c_2b_2+c_{p1}d_1-c_{p2}d_2)\dot{x}-\frac{1}{I_P}(c_1b_1^2+c_2b_2^2+c_{p1}d_1^2+c_{p2}d_2^2)\dot{\theta}-\frac{c_{p1}}{I_p}\dot{x}_{p1}+\frac{c_{p2}d_2}{I_p}\dot{x}_{p2}-\frac{c_1b_1}{I_p}\dot{x}_{t1}+\frac{c_2b_2}{I_p}\dot{x}_{t2}+\frac{1}{I_P}(f_1b_1-f_2b_2) \quad (2)$$

$$\ddot{x}_{p1}=\frac{1}{m_{p1}}(k_{p1}x+k_{p1}d_1\theta-k_{p1}x_{p1})+\frac{1}{m_{p1}}(c_{p1}\dot{x}+c_{p1}d_1\dot{\theta}-c_{p1}\dot{x}_{p1}) \quad (3)$$

$$\ddot{x}_{p2}=\frac{1}{m_{p2}}(k_{p2}x-k_{p2}d_2\theta-k_{p2}x_{p2})+\frac{1}{m_{p2}}(c_{p2}\dot{x}-c_{p2}d_2\dot{\theta}-c_{p2}\dot{x}_{p2}) \quad (4)$$

$$\ddot{x}_{t1}=\frac{1}{m_{t1}}(k_1x-k_1b_1\theta-(k_1+k_{t1})x_{t1}+k_{t1}y_1-F_{a1})+\frac{1}{m_{t1}}(c_1\dot{x}-c_1b_1\dot{\theta}-(c_1+c_{t1})\dot{x}_{t1}+c_{t1}\dot{y}_1) \quad (5)$$

$$\ddot{x}_{t2}=\frac{1}{m_{t2}}(k_2x-k_2b_2\theta-(k_2+k_{t2})x_{t2}+k_{t2}y_2-F_{a2})+\frac{1}{m_{t2}}(c_2\dot{x}-c_2b_2\dot{\theta}-(c_2+c_{t2})\dot{x}_{t2}+c_{t2}\dot{y}_2) \quad (6)$$

Where $I_P$is the mass moment of inertia for the vehicle body, m is the mass for the vehicle chassis/body, m_{t1} and m_{t2} are the un-sprung masses of the front and rear, respectively, x_p is the vertical displacement of vehicle body at the center of gravity, x_{p1} and x_{p2} are the vertical displacements of the front and rear passenger & seat displacements respectively, $\ddot{x}_{p1},\ddot{x}_{p2}$ are the front and rear passenger & seat accelerations, $\ddot{x}_{t1},\ddot{x}_{t2}$ are the front and rear tyre accelerations respectively. $\theta,\ddot{\theta}$ are the pitch motion and pitch acceleration of vehicle body at the center of gravity, F_{a1} and F_{a2} are front and rear actuators forces respectively, y_1 and y_2 are the front and rear irregular excitation from the road surfaces, a and b are the distances from the front and rear suspension locations respectively. The parameters of the vehicle model used in this article are reserved from [22] and given in Table 1.

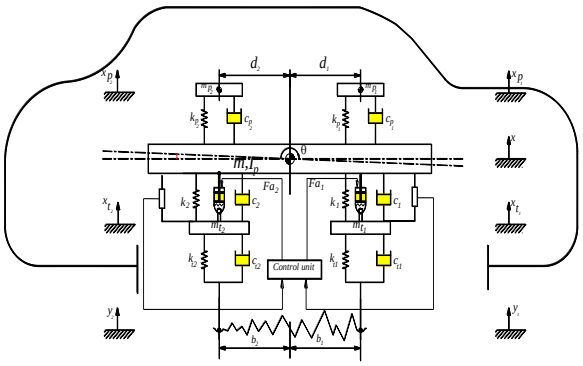

Fig. 1: Half vehicle suspension active model with 6 DoF

Table 1: Parameters of the vehicle model [24]

Parameter	Description	Unit	Value
I_P	Body inertia	kg.m^2	3443.05
m_{p1}	Driver mass	kg	75
m_{t1}	Front axle mass	kg	87.17
k_1	Front main stiffness	N/m	66824.2
k_2	Rear main stiffness	N/m	18615.0
kp_1	Front seat stiffness	N/m	14000
kp_2	Rear seat stiffness	N/m	14000
kt_1	Front tire stiffness	N/m	101115
kt_2	Rear seat stiffness	N/m	101115
b_1	Dimension	m	1.271
b_2	Dimension	m	0.481
m	Body mass	kg	17994.4
m_{p2}	Passenger mass	kg	14
m_{t2}	Rear axle mass	kg	140.
c_1	Front main damping	Ns/m	1190
c_2	Rear main damping	Ns/m	1000
c_{p1}	Front seat damping	Ns/m	50.2
c_{p2}	Rear seat damping	Ns/m	62.1
c_{t1}	Rear main damping	Ns/m	14.6
c_{t2}	Rear tire damping	Ns/m	14.6
b_2	dimension	Ns/m	1.713
d_2	dimension	Ns/m	1.313

3. Design of MOGA FOPID controller

This section offers a brief description of the FOPID controller, which was presented in [25] and applied in this article in an active manner. Fig. 2 shows the structure of the FOPID controller to enhance the ride comfort and vehicle stability. The most common formula of the FOPID is P $I^{\lambda}D^{\mu}$ containing integrator of order λ and a differentiator of order μ; where μ and λ can be any real number. The transfer function of the proposed FOPID controller realized through the Laplace transform is assumed as follows,

$$G_c = K_p + K_i \frac{1}{s^{\lambda}} + K_d s^{\mu} \ (\mu \text{ and } \lambda > 0) \qquad (7)$$

The values of the orders μ and λ along with K_p, K_i and K_d are the five unknown gains in the optimization problem that provides more possibility to recognize the optimum control performance. The error signal is the front and rear suspension working spaces.

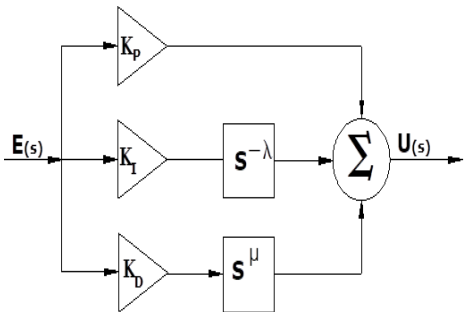

Fig. 2: Configuration model of FOPlD controller

The optimization problem consists of a vector of functions which varies from a single-objective optimization problem. The main aim of objective functions used in this paper is to tune the FOPID controller gains (λ $\mu K_p K_i K_d$). The gain crossover frequency (ω_{gc}) and the phase margin (ϕ_m) are selected as the two objectives for the optimization problem of the FOPID controller, i.e,

$$\text{Maximize } J_1 = \omega_{gc} \text{ and Maximize } J_2 = \phi_m \qquad (8)$$

It's clearly known that Eqn. (8) guarantees the stability of the controlled system under the drive of FOPID controller. The gain cross over frequency and phase margin of the controlled system are defined according to Eqn. (9) and Eqn. (10) respectively.

$$20 \log\left|C(j\omega_{cg})G(j\omega_{cg})\right| = 0 \text{ dB} \qquad (9)$$

$$\text{Arg}\left(C(j\omega_{cg})G(j\omega_{cg})\right) = -\pi + \emptyset_m \qquad (10)$$

The two objectives in Eqn. (8) must be maximized to enhance ride comfort and vehicle stability. High value of ω_{gc} operates the controlled system very fast. In order to perform the optimization algorithm to maximize the objectives in Eqn. (8), a set of constraints has been combined for the search with only those solutions.

Yielding positive gain margin and phase margin to offer good system stability. These constraints and their aims are identified as follows:-

1) To reject the high-frequency noise, let the closed loop transfer function have a small magnitude at specified frequency ω to be less than specified gain H as defined below,
$$\frac{C(j\omega)G(j\omega)}{1+C(j\omega)G(j\omega)}_{dB} \leq H \qquad (11)$$
2) To eliminate the steady state error, fractional integrator of order is implemented.
3) $k + \lambda$, $k \in N$, $0 < \lambda < 1$, as efficient as an integer order integrator of order $k + 1$.
4) Also, the merging between the frequency and time domain parameters through the minimization of the root mean square (RMS) of the front and rear suspension working spaces is needed to formulate the proposed FOPID controller.
5) To ensure the robustness of the system, rejection of the high frequencies is very important and can be performed using,
$$\frac{1}{1+C(j\omega)G(j\omega)}_{dB} \leq N \qquad (12)$$

Full details of FOPID controller design in frequency domain are explained in [26]. From the above objectives and constraints, a set of nonlinear equations, Eqns. (7) to (12) are obtained. The complexity of this set of nonlinear equations is very significant especially when it uses in a $PI^{\lambda}D^{\mu}$ controller and fractional orders of the Laplace variables are introduced. That is the reason why it is not trivial to solve this set of equations in an easy and direct way. So that, the MOGA is used to tune the five optimized controller gains using the N integer Toolbox under Matlab Software to apply fractional order controllers and evaluate their performance.

The main motivation for using MOGA to solve the present optimization problem is its ability to deal instantaneously with a set of possible solutions which provides numerous members of the Pareto-optimal set through a single run of the algorithm, rather than executing a series of separate runs as the traditional mathematical programming techniques which increases the traditional computational costs [27]. In the proposed FOPID controller, the arrangement in each unit transfer

function is taken as the main objective function to be minimized and the rest of conditions are taken as some constraints to achieve the minimization for each unit. All of them are subjected to the optimization parameters (λ, μ, K_p, K_i and K_d) defined using MOGA. Fig. 3 shows the arrangement of the proposed MOGA FOPID controller. After determining the lower and upper bounds of the controller gains, a number of individuals representing the candidate solutions are initialized in a random way. Then, the objective function is assessed for these individuals to get the fitness for each individual. Clearly, the optimization process contains the reproduction (competitive selection), crossover and mutation. If the optimization criteria are not achieved, the production of new generation will start. The MOGA parameters are presented in Table 2. The optimized values of controller gains are listed in Table 3.

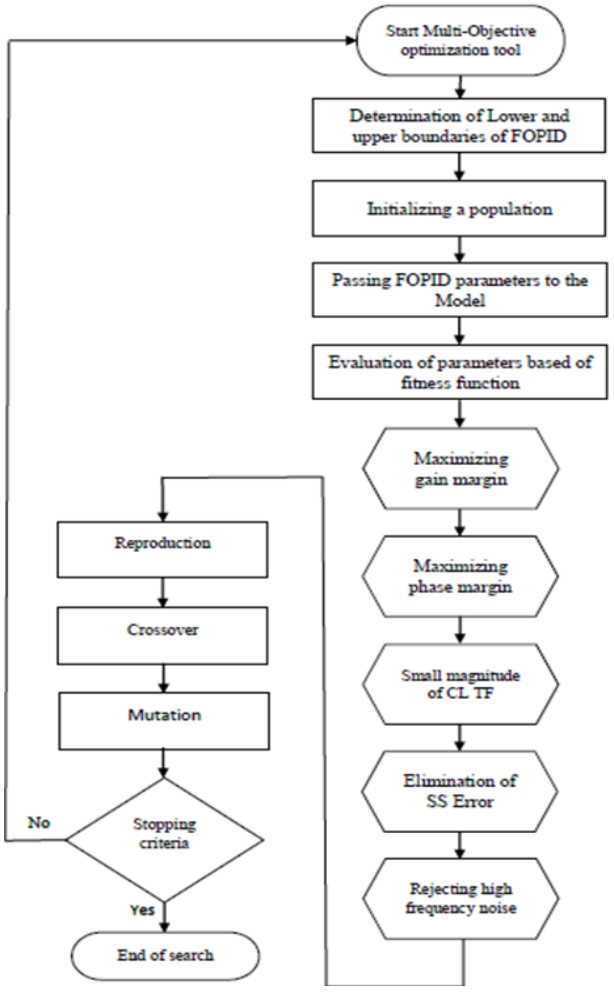

Fig. 3: Flow chart of genetic algorithm

Table 2: Genetic algorithm parameters

Genetic algorithm parameters	Value
Population size	200
Fitness scaling	Rank
Crossover technique	Constraint dependent
Crossover fraction	0.8
Mutation technique	Constraint dependent
Upper limit	[1000 100 0.95 500 0.95 1000 100 0.95 500 0.95]
Lower limit	[0 0 0 0 0 0 0 0 0 0]

Table 3: Initial & optimal values of FOPID controllers

Parameters	Initial Values	Optimal Values	Parameters	Initial Values	Optimal Values
K_{Pf}	1000	997.13	K_{Pr}	1000	673.031
K_{Df}	500	201.49	K_{Dr}	500	90
K_{If}	100	25.87	K_{Ir}	100	19.57681
λ_f	0.99	0.688	λ_r	0.95	0.2411
μ_f	0.99	0.893	μ_r	0.95	0.7276

4. Numerical simulation and results

In this section, simulations are conducted by using Matlab Simulink for investigating the performance of the active controlled half-vehicle model. A 6 DoF half-vehicle model is used to introduce the control techniques proposed in this paper. A well-known bump road excitation is used to evaluate the system response to evaluate the efficiency of the proposed FOPID controllers. The performance of the FOPID controller is compared against the passive system. The excitation is described by,

$$z = a(1 - \cos(\omega_r t)) \quad (13)$$

Where, a is the half of the bump amplitude (a = 3.5 cm) [28], $\omega_r = {}^{2\pi V}/_{D}$, (D = 0.8 m) is the width of bump, and V is the vehicle speed. In the bump excitation, the vehicle travels the bump with constant speed 3.08 km/h. Fig. 4 shows the time history of road bump excitation. Figs. 5 to 16 represent the simulation results of all system performance criteria under bump road excitation. From these results, it is obviously seen that the proposed FOPID controller can absorb the energy due to road bumps very well, can decrease the settling time, and can enhance both ride comfort and vehicle stability compared to the passive suspension system.

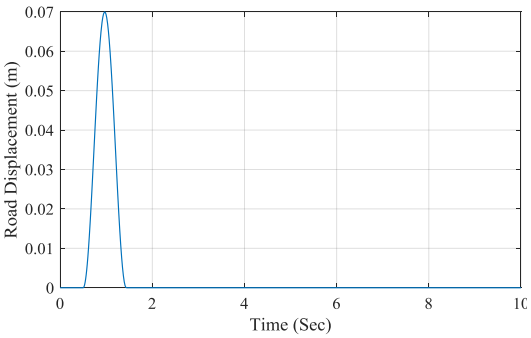

Fig. 4: Road profile

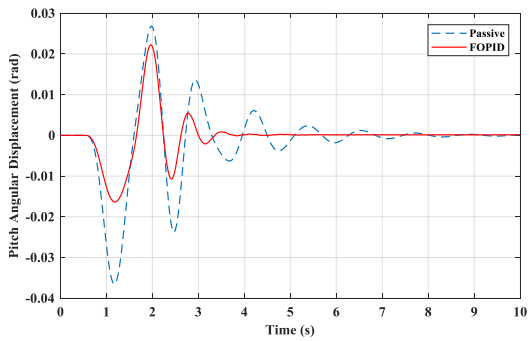

Fig. 5: Pitch angular displacement

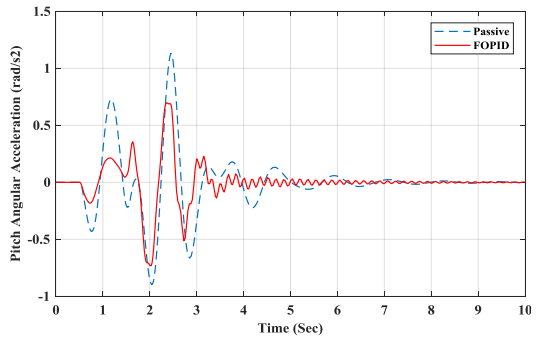

Fig. 6: Pitch angular acceleration

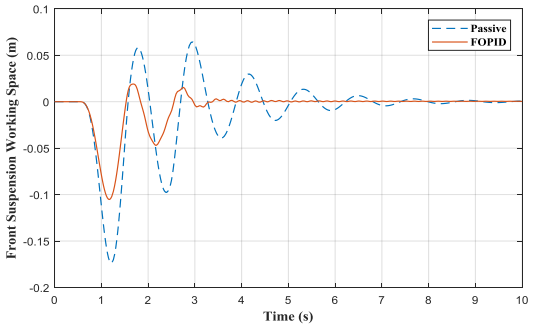

Fig. 7: Front suspension working space

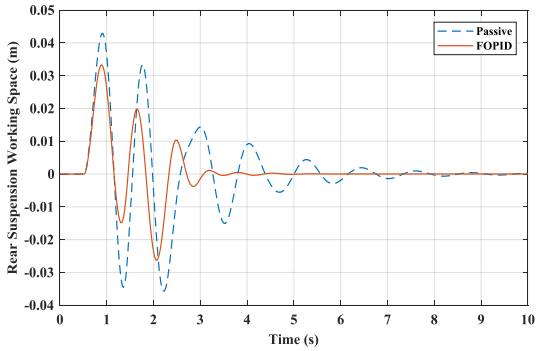

Fig. 8: Rear suspension working space

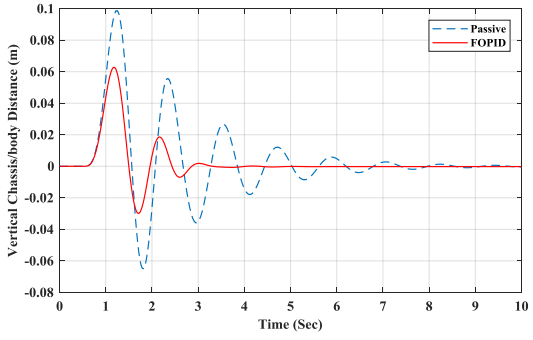

Fig. 9: Vertical chassis/body distance

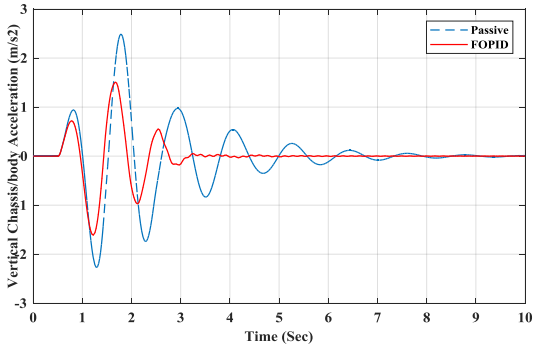

Fig. 10: Vertical chassis/body acceleration

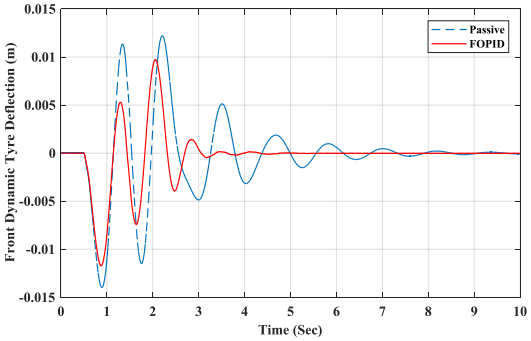

Fig. 11: Front dynamic tyre deflection

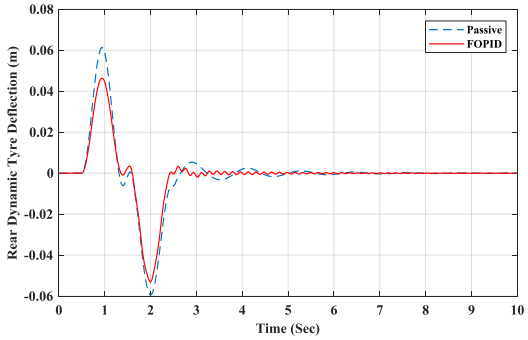

Fig. 12: Rear dynamic tyre deflection

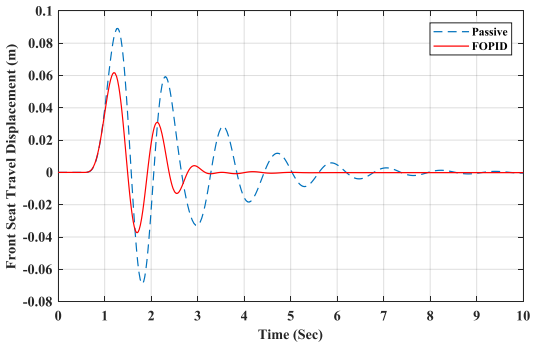

Fig. 13: Front seat travel displacement

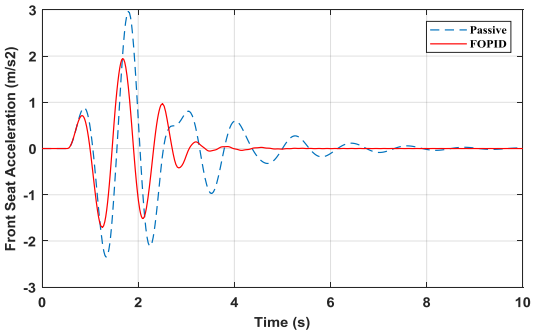

Fig. 14: Front seat acceleration

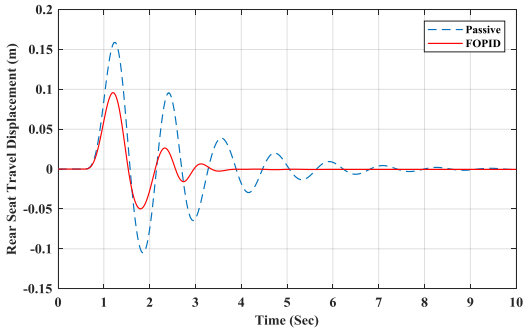

Fig. 15: Rear seat travel displacement

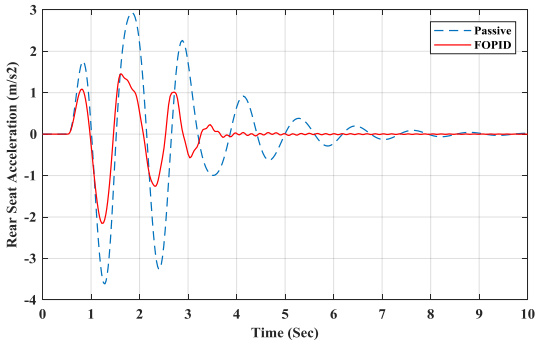

Fig. 16: Rear seat acceleration

Table 4 records a complete comparison between the active and passive systems showing the peak-to-peak (PTP) values and the percentage improvement of active compared to passive suspension. The proposed FOPID controller has the lowest peaks for all performance criteria, thereby demonstrating its effectiveness at enhancing ride comfort and vehicle stability.

Table 4: PTP values and improvement percentages

Parameter	Passive	Active	Improv. (%)
Pitch angular displacement (rad)	0.0634	0.0382	39
Pitch angular acceleration (rad/s^2)	2.0228	1.40	30.7
Front suspension working space (m)	0.2355	0.092	45
Rear suspension working space (m)	0.0766	0.04728	38.3
Vertical chassis/body distance (m)	0.1654	0.092	44.4
Vertical chassis/body acc. (m/s^2)	4.7136	3.056	35
Front dynamic tyre deflection (m)	0.0264	0.022	16.7
Rear dynamic tyre deflection (m)	0.1192	0.0987	17
Front seat travel displacement (m)	0.159	0.0983	38.2
Front seat acceleration (m/s^2)	6.525	3.578	45.2
Rear seat travel displacement (m)	0.2647	0.1463	44.7
Rear seat acceleration (m/s^2)	6.493	3.585	44

5. Conclusion

FOPID controllers are demonstrated to be very successful and generalized replacement of classical PID controllers due to their advantages. In this paper, an optimized FOPID controller is implemented to improve the overall performance of active vehicle suspension system using MOGA to tune controllers' gains. A half vehicle suspension system with 6 DoF incorporating two seats, front and rear was derived and simulated using Matlab/Simulink. The proposed FOPID active vehicle suspension was compared to passive suspension system under a well-known bump road disturbance in order to confirm the effectiveness of the proposed FOPID controller. The simulation results confirm that the proposed FOPID controller of active vehicle suspension offered a superior performance and can deal an excellent enhancement of the ride comfort and vehicle stability.

REFERENCES:

[1] A. Shojaei, H. Metered, S.Shojaei and S.O. Oyadiji. 2013. Theoretical and experimental investigation of magneto-rheological damper based semi-active suspension systems, *Int. J. Vehicle Structures & Systems*, 5(3-4), 109-120. http://dx.doi.org/10.4273/ijvss.5.3-4.06.

[2] H. Metered. 2010. *Modelling and Control of Magneto Rheological Dampers for Vehicle Suspension Systems*, PhD Thesis, School of Mech., Aerospace and Civil Engg., The University of Manchester, Manchester, UK.

[3] H. Metered. 2012. Application of nonparametric magneto rheological damper model in vehicle semi-active suspension system, *SAE Int. J. Passeng. Cars: Mech. Syst.*, 5(1), 715-726. https://doi.org/10.4271/2012-01-0977.

[4] H. Metered, A. Elsawaf, T. Vampola and Z. Sika. 2015. Vibration control of MR-damped vehicle suspension system using PID controller tuned by particle swarm optimization, *SAE Int. J. Passeng. Cars - Mech. Syst.* 8(2), 426-435. https://doi.org/10.4271/2015-01-0622.

[5] D.A. Crolla and M.B.A. Abdel-hady. 1991. Active suspension control; performance comparisons using control laws applied to a full vehicle model, *Vehicle System Dynamics*, 20(2), 107-120. https://doi.org/10.1080/00423119108968982.

[6] G. Priyandoko, M. Mailah and H. Jamaluddin. 2009. Vehicle active suspension system using skyhook adaptive neuro-active force control, *Mech. Systems and Signal Proc.*, 23(3), 855-868. https://doi.org/10.1016/j.ymssp.2008.07.014

[7] J. Wang, D.A. Wilson, W. Xu and D.A. Crolla. 2005. Active suspension control to improve vehicle ride and steady-state handling. *Proc. 44th IEEE Conf. Decision and Control and European Control Conf.*, Seville, Spain.

[8] A. Shehata, H. Metered, and W.A.H. Oraby. 2015. Vibration control of active vehicle suspension system using fuzzy logic controller, *Vibration Engg. and Tech. of Machinery*, 23, 389-399.

[9] Y.M. Sam, J.H. Osman and M.R.A.A. Ghani. 2004. A class of proportional-integral sliding mode control with application to active suspension system, *Systems & Control Letters*, 51(3-4), 217-223. https://doi.org/10.1016/j.sysconle.2003.08.007.

[10] K.A. Tahboub. 2005. Active nonlinear vehicle-suspension variable-gain control, *Intelligent Control, Proc. IEEE Int. Symp. Mediterrean Conf. Control and Automation, Limassol*, Cyprus.

[11] M.S. Kumar and S. Vijayarangan. 2006. Design of LQR controller for active suspension system, *Indian J. Engg., and Materials Sci.*, 13(3), 173-179.

[12] H. Li, J. Yu, C. Hilton and H. Liu. 2013. Adaptive sliding-mode control for nonlinear active suspension vehicle systems using T-S fuzzy approach, *IEEE Trans. Industrial Electronics*, 60(8), 3328-3338. https://doi.org/10.1109/TIE.2012.2202354.

[13] A.S. Emam. 2017. Active vibration control of automotive suspension system using fuzzy logic algorithm, *Int. J. Vehicle Structures & Systems*, 9(2), 77-82. http://dx.doi.org/10.4273/ijvss.9.2.03.

[14] H. Metered, M. Kozek and Z. Šika. 2015. Vibration control of active vehicle suspension using fuzzy based sliding surface, *Int. J. Fuzzy Systems and Advanced Applications*, 2, 41-48.

[15] A.S. Emam and A.M.A. Ghany. 2010. Enhancement of ride quality of a quarter cars by using h_∞ design of a robust LMI output feedback controller, *Ain Shams J. Mech. Engg.*, 2, 35-43.

[16] R. Wang, H. Jing, H.R. Karimi and N. Chen. 2015. Robust fault-tolerant H_∞ control of active suspension systems with finite-frequency constraint, *Mech. Systems and Signal Proc.*, 62-63, 341-355. https://doi.org/10.1016/j.ymssp.2015.01.015.

[17] A.S. Emam and A.M. Abdel Ghany. 2012. Enhancement of ride quality of quarter vehicle model by using mixed

h_2/h_∞ with pole-placement, *Engg.*, 4(2), 126-132. https://doi.org/10.4236/eng.2012.42016.

[18] A.S. Emam. 2015. Fuzzy self-tuning of PID controller for active suspension system, *Adv. in Powertrains and Automotive*, 1(1), 34-41. https://doi.org/10.12691/apa-1-1-4.

[19] H. Khodadadi and H. Ghadiri. Self-tuning PID controller design using fuzzy logic for half car active suspension system, *Int. J. Dynam. Control*, 6(1), 224-232.

[20] H. Metered, W. Abbas and A.S. Emam. Optimized proportional integral derivative controller of vehicle active suspension system using genetic algorithm, *SAE Tech. Paper 2018-01-1399*. https://doi.org/10.4271/2018-01-1399.

[21] A.A. Zamani, S. Tavakoli and S. Etedali. 2017. Fractional order PID control design for semi-active control of smart base - isolated structures: A multi-objective cuckoo search approach. *ISA Trans.*, 67, 222-232. https://doi.org/10.1016/j.isatra.2017.01.012.

[22] J. Zhang and Y. Zhang. 2008. Fractional-order PID control and optimization for vehicle active steering, *Proc. 7th World Congress on Intelligent Control and Automation*, Chongqing, China.

[23] X. Dong, D. Zhao, B. Yang and C. Han. 2016. Fractional-order control of active suspension actuator based on parallel adaptive clonal selection algorithm, *J. Mech. Sci. and Tech.* 30(6), 2769-2781. https://doi.org/10.1007/s12206-016-0538-2

[24] H.D. Taghirad and E. Esmailzadeh. 1998. Automobile passenger comfort assured through LQG/LQR active suspension, *J. Vibration and Control*, 4, 603-618. https://doi.org/10.1177/107754639800400504.

[25] S. Gad, H. Metered, A. Bassuiny and A.M.A. Ghany. 2017. Multi-objective genetic algorithm fractional-order PID controller for semi-active magnetorheologically damped seat suspension, *J. Vibration and Control*, 23(8), 1248-1266. https://doi.org/10.1177/1077546315591620.

[26] S. Das, S. Saha, S. Das and A. Gupta. 2011. On the selection of tuning methodology of FOPID controllers for the control of higher order processes, *ISA Trans*, 50(3), 376-388. https://doi.org/10.1016/j.isatra.2011.02.003.

[27] J.L. Cohon. 1978. *Multi-objective Programming and Planning*, Academic Press, New York.

[28] S.Y. Moon and W.H. Kwon. 1998. Genetic-based fuzzy control for half-car active suspension systems, *Int. J. Systems Science*, 29, 699-710. https://doi.org/10.1080/00207729808929564.